

Spin-phase transition in an array of quantum rings controlled by cavity photons

Vidar Gudmundsson,^{1,*} Vram Mughnetsyan,^{2,†} Hsi-Sheng Goan,^{3,4,5,‡} Jeng-Da Chai,^{3,4,5,§}
Nzar Rauf Abdullah,^{6,¶} Chi-Shung Tang,^{7,**} Valeriu Moldoveanu,^{8,††} and Andrei Manolescu^{9,‡‡}

¹*Science Institute, University of Iceland, Dunhaga 3, IS-107 Reykjavik, Iceland*

²*Department of Solid State Physics, Yerevan State University, Alex Manoogian 1, 0025 Yerevan, Armenia*

³*Department of Physics and Center for Theoretical Physics,
National Taiwan University, Taipei 106319, Taiwan*

⁴*Center for Quantum Science and Engineering, National Taiwan University, Taipei 106319, Taiwan*

⁵*Physics Division, National Center for Theoretical Sciences, Taipei 106319, Taiwan*

⁶*Physics Department, College of Science, University of Sulaimani, Kurdistan Region, Iraq*

⁷*Department of Mechanical Engineering, National United University, Miaoli 360302, Taiwan*

⁸*National Institute of Materials Physics, PO Box MG-7, Bucharest-Magurele, Romania*

⁹*Department of Engineering, Reykjavik University, Menntavegur 1, IS-102 Reykjavik, Iceland*

We model a spin-phase transition in a two-dimensional square array, or a lateral superlattice, of quantum rings in an external perpendicular homogeneous magnetic field. The electron system is placed in a circular cylindrical far-infrared photon cavity with a single circularly symmetric photon mode. Our numerical results reveal that the spin ordering of the two-dimensional electron gas in each quantum ring can be influenced or controlled by the electron-photon coupling strength and the energy of the photons. The Coulomb interaction between the electrons is described by a spin-density functional approach, but the para- and the diamagnetic electron-photon interactions are modeled via a configuration interaction formalism in a truncated many-body Fock-space, which is updated in each iteration step of the density functional approach. In the absence of external electromagnetic pulses this spin-phase transition is replicated in the orbital magnetization of the rings. The spin-phase transition can be suppressed by a strong electron-photon interaction. In addition, fluctuations in the spin configuration are found in dynamical calculations, where the system is excited by a time-dependent scheme specially fit for emphasizing the diamagnetic electron-photon interaction.

I. INTRODUCTION

Researchers have been exploring and modeling [1–4] the effects of placing chemical systems [5], molecules [6], and nanoscale electron systems in photon cavities [7, 8] in order to modify or control their properties. On the theoretical side, several methods have been used, some being gathered under the umbrella concept of quantum electrodynamic density functional theory (QEDFT) [9–12].

Concurrently, this interest has been extended to large systems with two-dimensional electron gas (2DEG) in heterostructures. Experiments have indicated that the 2DEG in GaAs heterostructures is especially advantageous for fundamental research on the 2DEG-cavity photon interactions due to its high purity and polarizability [13, 14].

The free homogeneous 2DEG placed in a parallel plate cavity has been modeled [15–17], as well as the 2DEG modulated in a superlattice and subjected to the static electronic Coulomb interaction, both in the static [18–

20], or in the dynamic case after short excitation pulse [21, 22].

Previously, the present group of researchers has modeled the modulated 2DEG in a square array of quantum dots interacting with the quantized TE₀₁₁ mode of a circular cylindrical cavity. That was done in order to strengthen the diamagnetic electron-photon interaction of the system placed in a homogeneous external magnetic field promoting persistent circular or rotational currents. The model calculations were accomplished for the static system using the quantum electrodynamic density functional theory tensor product (QED-DFT-TP) formalism presented by Malave *et al.* [11] adapted to the 2DEG and the external magnetic field [20]. Particularly, the excitations of the system with a short pulse-formed modulation of the electron-photon interaction in a self-consistent real-time approach showed how diamagnetic two-photon transitions are strongly promoted in the system [22].

This has directed us to consider a system with the 2DEG in a superlattice of quantum rings. There are two reasons for the present study: i) the ring array may be more susceptible to the symmetry of the TE₀₁₁ mode of a cylindrical cavity, and ii) the exchange correlations between the rings may play a special role in the system. This last point is supported by our earlier findings for the dot system, i.e. an array of quantum dots, where the results of the calculations using the QED-DFT-TP [20], or the QEDFT [18] clearly show that, an increased electron-photon interaction weakens the Coulomb exchange interactions considerably. Last but not least, we believe that

* vidar@hi.is

† vram@ysu.am

‡ goan@phys.ntu.edu.tw

§ jdchai@phys.ntu.edu.tw

¶ nzar.r.abdullah@gmail.com

** cstang@nuu.edu.tw

†† valim@infim.ro

‡‡ manoles@ru.is

a quantum ring array is a suitable platform to further test the QED-DFT-TP method.

The paper is organized as follows: In Sec. II we briefly describe the model, which was already introduced in our previous works. The results and discussion thereof are found in Sec. III, with the conclusions drawn in Sec. IV. Appendix A contains technical details of the methodology used for the modeling.

II. MODEL

The mutual Coulomb interaction of the electrons in the 2DEG are described within spin density functional theory using an exact direct term, and approximate exchange correlations terms detailed in the Appendix of Ref. [18]. The extension to systems in homogeneous external magnetic field was presented by Lubin *et al.* and Koskinen *et al.* [23, 24] and built on development by Barth and Hedin [25], and Tanatar and Ceperley [26]. The 2DEG in the xy -plane is in an external homogeneous magnetic field $\mathbf{B} = B\mathbf{e}_z$ described by the vector potential $\mathbf{A} = (B/2)(-y, x)$. The external magnetic field introduces the natural length scale, the magnetic length $l = (\hbar c/(eB))^{1/2}$, and an energy scale, the cyclotron energy $\hbar\omega_c = (eB/(m^*c))$.

The potential defining the square array, or lateral superlattice, of rings is

$$V_{\text{per}}(\mathbf{r}) = -V_0 \left[\sin\left(\frac{g_1 x}{2}\right) \sin\left(\frac{g_2 y}{2}\right) \right]^2 + V_0 \left[\sin\left(\frac{g_1 x}{2}\right) \sin\left(\frac{g_2 y}{2}\right) \right]^4, \quad (1)$$

with $V_0 = 64.0$ meV. The potential is displayed in Fig. 1 for 4 unit cells of the extended superlattice hosting the 2DEG. The square superlattice of quantum rings is

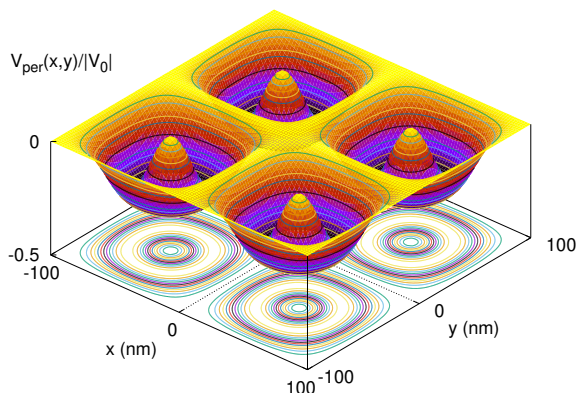


FIG. 1. Four unit cells of the potentials defining the two-dimensional array of quantum rings. The superlattice length $L = 100$ nm.

spanned by the spatial vectors $\mathbf{R} = n\mathbf{l}_1 + m\mathbf{l}_2$ with $n, m \in$

\mathbf{Z} , where the unit vectors are $\mathbf{l}_1 = L\mathbf{e}_x$ and $\mathbf{l}_2 = L\mathbf{e}_y$. The reciprocal lattice is spanned by $\mathbf{G} = G_1\mathbf{g}_1 + G_2\mathbf{g}_2$ with $G_1, G_2 \in \mathbf{Z}$ and its unit vectors $\mathbf{g}_1 = 2\pi\mathbf{e}_x/L$ and $\mathbf{g}_2 = 2\pi\mathbf{e}_y/L$. The period of the superlattice is $L = 100$ nm, setting another length scale competing with the magnetic length l [27].

The 2DEG is placed in the center of a circular cylindrical FIR photon cavity. The long wavelength approximation for the vector potential for the TE_{011} cavity photon mode was derived in the Appendix of Ref. [20] to be

$$\mathbf{A}_\gamma(\mathbf{r}) = \mathbf{e}_\phi \mathcal{A}_\gamma (a_\gamma^\dagger + a_\gamma) \left(\frac{r}{l}\right), \quad (2)$$

where \mathbf{e}_ϕ is the unit angular vector for the polar coordinates, (r, ϕ) . The vector potential (2) exhibits the same spatial form as the vector potential \mathbf{A} of the external homogeneous magnetic field $\mathbf{B} = B\mathbf{e}_z$ [20]. a_γ^\dagger and a_γ are the photon creation and annihilation operators of the FIR cavity photon mode, respectively.

The electrons of the 2DEG interact with the cavity photon mode according to

$$H_{\text{int}} = \frac{1}{c} \int_{\mathbf{R}^2} d\mathbf{r} \mathbf{J}(\mathbf{r}) \cdot \mathbf{A}_\gamma(\mathbf{r}) + \frac{e^2}{2m^*c} \int_{\mathbf{R}^2} d\mathbf{r} n_e(\mathbf{r}) A_\gamma^2(\mathbf{r}), \quad (3)$$

where both the para- and the diamagnetic parts of the electron-photon interaction are accounted for. In the static part of the calculations the electron and the current densities are defined as

$$n_e(\mathbf{r}) = \frac{1}{(2\pi)^2} \sum_{\alpha\sigma} \int_{-\pi}^{\pi} d\theta |\psi_{\alpha\theta\sigma}(\mathbf{r})|^2 f(E_{\alpha\theta\sigma} - \mu), \quad (4)$$

$$\mathbf{J}_i(\mathbf{r}) = \frac{-e}{m^*(2\pi)^2} \sum_{\alpha\sigma} \int_{-\pi}^{\pi} d\theta \Re \{ \psi_{\alpha\theta\sigma}^*(\mathbf{r}) \pi_i \psi_{\alpha\theta\sigma}(\mathbf{r}) \} f(E_{\alpha\theta\sigma} - \mu), \quad (5)$$

respectively, for $i = x$ or y . f notes the equilibrium Fermi distribution, μ is the chemical potential of the electron system, and

$$\boldsymbol{\pi} = \left(\mathbf{p} + \frac{e}{c} \mathbf{A} \right). \quad (6)$$

The wavefunctions $\psi_{\alpha\theta\sigma}$ correspond to the states $\{|\alpha\theta\sigma\rangle\}$ of the self-consistently diagonalized static Hamiltonian of the electron-photon system with the energy spectrum $E_{\alpha\theta\sigma}$.

In the Appendix of Ref. [20] the electron-photon interaction (3) is rewritten in terms of the photon creation and annihilation operators as

$$H_{\text{int}} = g_\gamma \hbar\omega_c \{ lI_x + lI_y \} (a_\gamma^\dagger + a_\gamma) + g_\gamma^2 \hbar\omega_c \mathcal{N} \left\{ \left(a_\gamma^\dagger a_\gamma + \frac{1}{2} \right) + \frac{1}{2} (a_\gamma^\dagger a_\gamma^\dagger + a_\gamma a_\gamma) \right\}, \quad (7)$$

where conveniently and importantly, the constants I_x , I_y , and \mathcal{N} turn out as functionals the electron charge- and current densities. Previous calculations with the model for a square array of quantum dots interacting with the TE₀₁₁ cylindrical mode show the importance of retaining all the terms of the diamagnetic part of the interaction, the second line in Eq. (7) [22]. The dimensionless electron-photon coupling constant emerging in the derivation is

$$g_\gamma = \left\{ \left(\frac{e\mathcal{A}_\gamma}{c} \right) \frac{l}{\hbar} \right\}. \quad (8)$$

The energy of the photons in the single cavity mode is $E_\gamma = \hbar\omega_\gamma$.

In order to explore the dynamical evolution of the system, it is excited with a short pulse-like modulation of the electron-photon interactions.

$$H_{\text{ext}}(t) = F(t) \left[g_\gamma \hbar\omega_c \{lI_x + lI_y\} (a_\gamma^\dagger + a_\gamma) \right. \\ \left. + g_\gamma^2 \hbar\omega_c \mathcal{N} \left\{ \left(a_\gamma^\dagger a_\gamma + \frac{1}{2} \right) + \frac{1}{2} (a_\gamma^\dagger a_\gamma^\dagger + a_\gamma a_\gamma) \right\} \right] \quad (9)$$

with

$$F(t) = \left(\frac{V_t}{\hbar\omega_c} \right) (\Gamma t)^2 \exp(-\Gamma t) \cos(\omega_{\text{ext}} t). \quad (10)$$

The time-evolution of the system is calculated self-consistently with the Liouville-von Neumann equation for the density, or the probability, operator $\rho^\theta(t)$ for each θ -point in the first Brillouin zone of the reciprocal lattice.

$$i\hbar\partial_t \rho^\theta(t) = [H[\rho^\theta(t)], \rho^\theta(t)]. \quad (11)$$

That is possible as, neither any term in the electron-photon interaction (7), nor the excitation (9) couple different θ points in the reciprocal lattice. Self-consistency refers to that the direct Coulomb and the exchange-correlation functionals, depending on the electron density, have to be updated in each iteration within each time step together with the functionals I_x , I_y , and \mathcal{N} of the electron charge- and current densities. The total time-dependent Hamiltonian $H[\rho^\theta(t)]$ is a functional of the time-dependent density operators $\rho^\theta(t)$ and it is also an explicit function of time through (10). It includes the periodic ring potential (1), the electron-photon interaction (7), the electron Coulomb direct and exchange-correlation terms, the Zeeman spin energy term, the time-dependent modulation of the electron-photon interaction (9-10), and the electron and photon ‘‘kinetic terms’’ [22]. Subsequently, the time-dependent electron and current densities have to be calculated from the density operator instead of the Fermi distribution as the excitation throws the system out of equilibrium [22].

For the dynamic system we calculate the time-dependent mean photon number

$$N_\gamma(t) = \frac{1}{(2\pi)^2} \sum_\sigma \int_{-\pi}^{\pi} d\theta \text{Tr} \{ \rho_\sigma^\theta(t) a_\gamma^\dagger a_\gamma \} \quad (12)$$

and the time-dependent mean orbital magnetization

$$M_o(t) = \frac{1}{2c\mathcal{A}} \int_{\mathcal{A}} d\mathbf{r} (\mathbf{r} \times \langle \mathbf{J}(\mathbf{r}, t) \rangle) \cdot \mathbf{e}_z. \quad (13)$$

with $\mathcal{A} = L^2$. In previous publications we have used the notation Q_J for the orbital magnetization to emphasize its connection to a moment of the current density. In addition we evaluate the time-dependent spin magnetization

$$M_s(t) = -\frac{g\mu_B^*}{\mathcal{A}} \int_{\mathcal{A}} d\mathbf{r} \langle \sigma_z(\mathbf{r}, t) \rangle, \quad (14)$$

with σ_z identified as $\zeta = (n_\uparrow - n_\downarrow)/n_e$, the spin polarization defined in the spin-DFT formalism. $n_e = (n_\uparrow + n_\downarrow)$.

The integrand in Eq. (12) can be used to calculate the photon density in the first Brillouin zone of the reciprocal space

$$n_\gamma(\theta_1, \theta_2) = \langle a_\gamma^\dagger a_\gamma \rangle^\theta \quad (15)$$

for the static or the dynamical system. In the dynamical case the average, or the mean value, is taken with respect to the density operators as in Eq. (12) which can be reduced to diagonal operators in the static system, see Ref. [20].

III. RESULTS

For the model calculations, we assume GaAs parameters: the effective electron mass $m^* = 0.067m_e$, the dielectric constant $\kappa = 12.4$, and the effective g -factor $g^* = -0.44$. The magnetic flux through a unit cell comes from the commensurability condition $B\mathcal{A} = BL^2 = pq\Phi_0$ with the integers p and q [28–30], and the flux quantum $\Phi_0 = hc/e$. For the excitation pulse (10) we use $\hbar\omega_{\text{ext}} = 3.5$ meV, $\hbar\Gamma = 0.5$ meV, and $V_t/\hbar\omega_c = 0.8$.

A. Two electrons in each ring, $N_e = 2$

Figure 2 shows mostly expected results for 2 electrons in each ring. The total energy E_{tot} increases with increasing electron-photon coupling g_γ (a) and the same can be said about the photon number in each ring N_γ (b). There is a more subtle change in the orbital magnetization M_o (c) at low photon energy E_γ due to the varying occupation of the first photon replica. Importantly, we notice almost no change in the spin-configuration, seen through the spin magnetization (d), but a comparison of the results for the array of rings to the results for an array of dots for the same lattice size, $L = 100$ nm, makes immediately clear one fundamental difference. In the array of rings the Coulomb exchange interaction is stronger than for the dot array. It is sufficient to look at Fig. 2(d) in Ref. [20] showing the spin magnetization for $N_e = 2$ at the magnetic flux $pq = 2$, corresponding to the magnetic

field $B = 0.827$ T. It is very close to 0 for photon energies 1.0 and 2.0 meV and the dimensionless electron-photon coupling g_γ in the range from almost 0 to 0.3. Therefore, the spin configuration of each dot is a singlet state. For individual dots it has been known for a long time that the singlet state preferred by the system at low magnetic field changes to a triplet as the magnetic field is increased [31]. Note though, that in the calculations for a single dot a positive background charge is usually not assumed, so the direct Coulomb interaction is stronger than in an array, where a positive background charge is assumed. Figure 2 (in the present paper) shows the total energy E_γ , the mean photon number N_γ , the orbital M_o , and the spin magnetization M_s per unit cell for $pq = 2$ and $N_e = 2$. The spin magnetization in Fig. 2(d) shows that the two electrons in each ring are in a spin triplet state, even for very high electron-photon coupling. We find the same happening for the lower magnetic flux $pq = 1$ (not shown here) for the array of rings, the electrons remain in the triplet spin state.

For the dot system, i.e. an array of quantum dots, all our previous calculations using the QED-DFT-TP [20], or the QEDFT [18] show clearly that within the parameter range used here, the increased electron-photon interaction weakens the Coulomb exchange interactions considerably.

Below, we check better the static and dynamic properties of the ring array with $N_e = 2$ and $pq = 2$ flux quanta flowing through the unit cell before analyzing the situation for $N_e = 3$.

After the same dynamical excitation (9) as is used in Ref. [22] the mean photon number oscillates as is displayed in Fig. 3 for $g_\gamma = 0.08$ in (a), and 0.10 in (b). The oscillations are similar as for the quantum dot array, except for the observation that the excitation of the ring array looks to be more effective. That is not surprising as the active states of the ring system, in a polar coordinate system not used here, have mainly contributions from the eigenstates of the angular momentum operator for finite angular momentum, $M \neq 0$. In a quantum dot the ground state has a higher contribution from a state with zero angular momentum, the $M = 0$ state, in polar coordinates, that is less susceptible to a circular symmetric excitation. In polar coordinates M is the angular momentum quantum number.

The Fourier power spectra for the two-electron rings are displayed in Fig. 4. The only difference between the excitation spectra is that in Fig. 4(a) the coupling $g_\gamma = 0.08$, but it is 0.10 in (b). We notice the peaks are not at the bare photon energies, but are shifted proportionally to the electron-photon coupling g_γ . This interaction shift is exactly the reason for which excitation peak is best excited by the frequency spectrum the excitation forces on the system [22]. The spectrum of the excitation is the same for Fig. 4(a) and (b).

B. Three electrons in each ring, $N_e = 3$

Here, we will analyze the array of quantum rings with $N_e = 3$ electrons in each ring and $pq = 2$ flux quanta through the unit cell. First, in Fig. 5 we observe through the electron density (a) and the photon induced change of it (b), that we are dealing with a ring formed electron system in each unit cell of the superlattice. In addition, we see the distribution of the photons in the first Brillouin zone of the reciprocal space (c). The same is true for two electrons at $pq = 2$. The ring structure is not as clear for 2 or 3 electrons at the lower magnetic flux $pq = 1$. There, the hole in the center of the charge distribution is not quite as deep as for $pq = 2$. That can be explained by the magnetic length l , that is 28.21 nm at $pq = 2$, but 39.89 at $pq = 1$. We notice in Fig. 5(b) that the electron density is polarized radially outwards as the electron-photon coupling is increased. This is in accordance with our results for dot arrays, both in the QEDFT [18] and the QED-DFT-TP [20] formalism. Of course, the symmetry of the square array can distort the charge polarization, we see a slight indication of that here.

The electron density seen in Fig. 5 suggests that the inter-ring Coulomb exchange is strengthened for an array of rings due to the ‘‘closer spacing’’ of rings than dots for few electrons, and interestingly, increased electron-photon coupling slightly reduces the effective distance between the rings, if it is measured as the distance between the maxima in the charge distribution of the rings.

Figure 6 shows the total energy E_{tot} , the mean photon number N_γ , the orbital M_o , and the spin magnetization M_s per unit cell for $pq = 2$ and $N_e = 3$. Figure 6 should be compared to Fig. 2 for two electrons in each ring. We observe a clear phase change from the fully spin polarized state to a phase of single unpaired spins in each ring, when either the photon energy E_γ , or the electron-photon coupling g_γ is increased for low photon energy. Signs of this phase change in the static ring array are seen in all the variables displayed in Fig. 6, though they are clearest in subfigure (d) for the spin magnetization M_s .

We have done a calculation for the lower magnetic flux of $pq = 1$ for 3 electrons. There, for all values of the photon energy, we find the system to be maximally spin polarized for low electron-photon coupling, but for all other values of higher coupling, only a single unpaired spin is found in each ring.

These signs of a spin-phase transition in the static system open the question if any signs of it can be observed in the dynamic evolution of the system after an excitation. Indeed, signs can be found. The excitation of the array of quantum rings should not promote a change in the mean spin configuration. It can change the mean total orbital momentum, or the orbital magnetization in each ring with the induced circular electric field, but the spin should be conserved, but the mean spin in each ring might fluctuate around its original value. This is indeed what happens as can be seen in Fig. 7 for $g_\gamma = 0.08$.

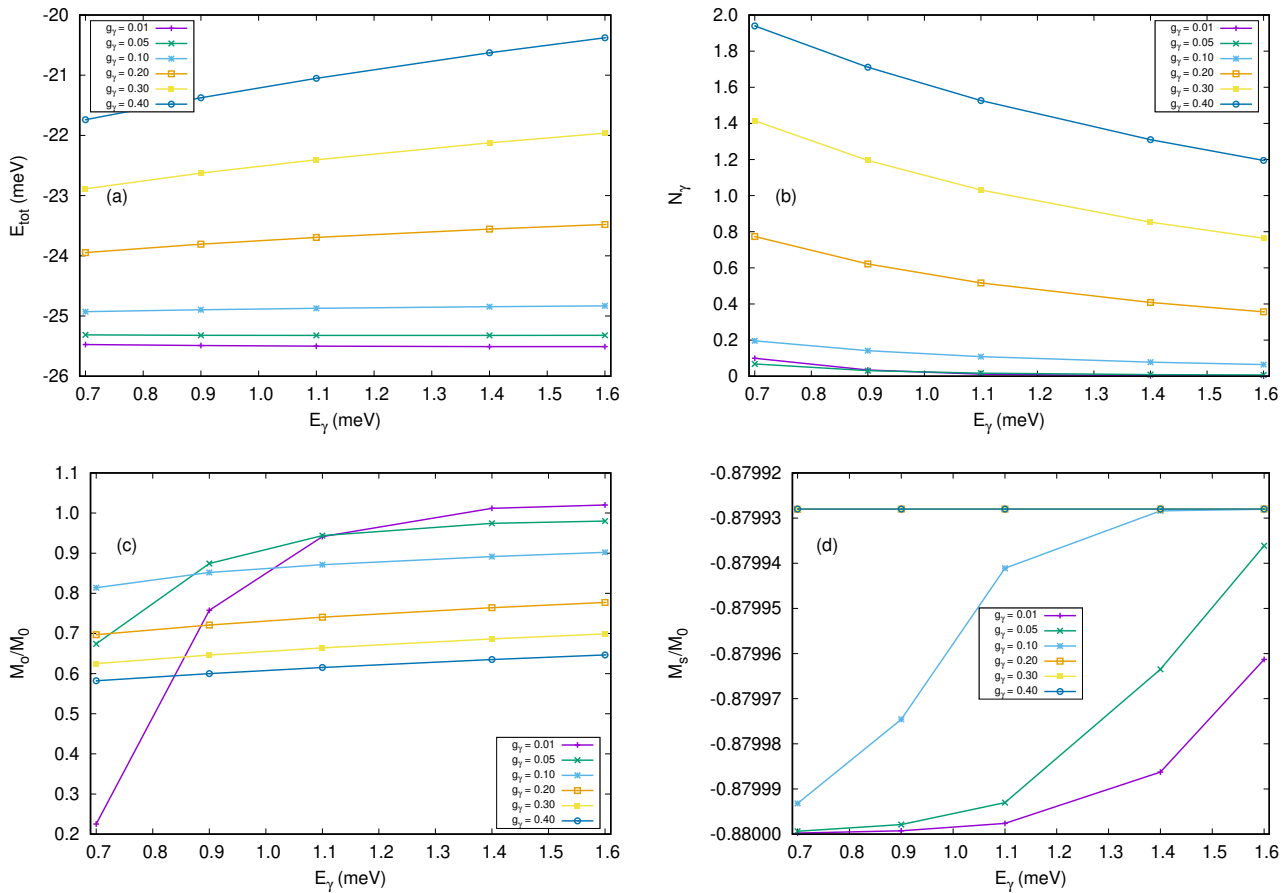


FIG. 2. The total energy E_{tot} (a), the mean number of photons N_γ (b), the orbital magnetization M_o (c), and the spin magnetization M_s (d) of the 2DEG in a unit cell as function of the photon energy E_γ for different values of the dimensionless electron-photon coupling g_γ . $T = 1.0$ K, $N_e = 2$, $pq = 2$, and $M_0 = \mu_B^*/L^2$.

Additionally, we see a slight trend to a period doubling in the orbital magnetization, reflecting an increase of the higher order transitions being activated.

The same behavior with more extremes can be seen for the case of the stronger electron-photon coupling $g_\gamma = 0.10$ displayed in Fig. 8.

In Fig. 9 this is compared for the total energy and the spin-magnetization for two different values of the photon energy, and three values of the electron-photon coupling. It is particularly interesting to see the difference in the spin-magnetization in subfigure (c). For the low electron-photon coupling of $g_\gamma = 0.06$ no fluctuations are seen on the scale used to capture the fluctuations for the other values of the coupling.

We stress that the fluctuations in the spin magnetization only show excitation peaks in the same energy locations as the mean photon number and the dynamic orbital magnetization. This reflects the fact that the chosen excitation can not exert any torque on the spins.

We specially note that we do not observe any formation of a spin density wave in the angular direction within one quantum ring, neither in the static nor in the dynamic

system. The total energy in Fig. 7(a), 8(a), and 9(a) and (b) is not totally constant after the excitation pulse ends at $t = 16$ ps. This has to be understood in relation with the Heisenberg uncertainty laws. The average of the total energy oscillates around a constant value. The number of electrons within a unit cell of the periodic system and the trace of the density matrices in each point θ retain their correct values with 11 to 12 significant digits.

IV. CONCLUSIONS

We have used a QED-DFT-TP formalism to describe the Coulomb interaction and a CI approach for both the para- and the diamagnetic electron-photon interactions for a 2DEG in a large superlattice of quantum rings embedded in a cylindrical FIR-photon cavity in an external magnetic field.

We find that in the ring array the Coulomb exchange interaction is stronger than in the corresponding array of quantum dots. For two electrons in each dot we observe a spin triplet state in each ring, even at low magnetic

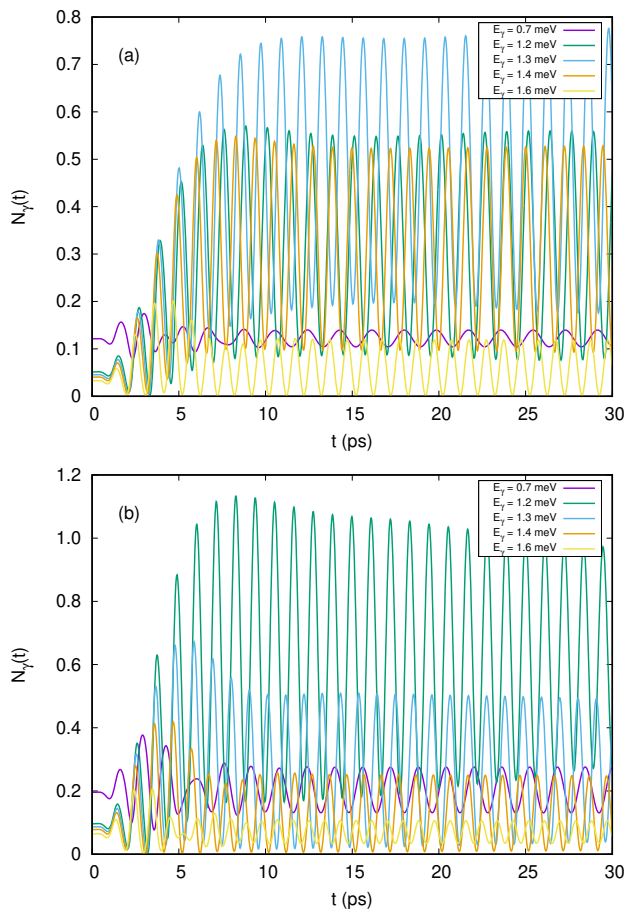


FIG. 3. The dynamic mean photon number $N_\gamma(t)$ per unit cell of the 2DEG as a function of time for the first 30 ps for different values of the photon energy E_γ and $g_\gamma = 0.08$ (a), and the electron-photon coupling $g_\gamma = 0.10$ (b). $N_e = 2$, $pq = 2$.

field.

For three electrons and two magnetic flux quanta $pq = 2$ in each ring cell we find a fully spin polarized state for the static system for low electron-photon coupling and small photon energy. As the electron-photon coupling, or the photon energy, are increased a phase transition to a single unpaired spin in each cell is observed in the superlattice. For a single magnetic flux quantum $pq = 1$ through the unit cell we observe the same kind of a spin-phase transition with respect to the strength of the electron-photon coupling, whereas a change in the photon energy in the range we use does not lead to a phase transition.

In the system with $pq = 2$ and two electrons in each ring a dynamical excitation of the system does not change its spin configuration, but tiny oscillations in the mean spin magnetization, most often just close to the numerical noise level, can be observed. The same could be said for all our former calculations for the excitation of arrays of quantum dots within the same formalism. The excitation does not affect the spin degree of freedom as analytical

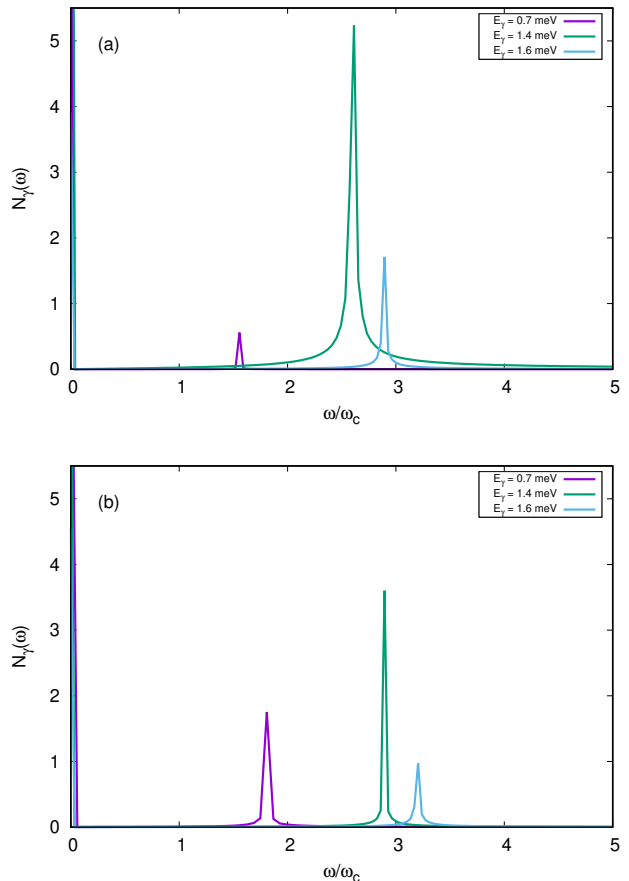


FIG. 4. The Fourier power spectra of the mean photon number per unit cell $N_\gamma(\omega)$ for different values of the photon energy E_γ and the electron-photon coupling $g_\gamma = 0.08$ (a), and $g_\gamma = 0.10$ (b). $N_e = 2$, $pq = 2$, and $\hbar\omega_c = 1.429$ meV.

evaluations show, but only the population of different states. For the 3-electron rings in the $pq = 2$ magnetic flux, we observe spin fluctuations in the system close to a phase transition, even though the mean spin value is conserved.

We observe thus, directly a spin-phase transition in the static system, but in the dynamical system we see the fluctuations that are known to be present in systems close to phase transitions. Both these phenomena support the idea that the superlattice, or array, of rings shows in this case a genuine spin-phase transition, and that the inter-ring exchange interaction is at work. Furthermore, the spin-phase transition can be suppressed by a strong electron-photon interaction. This suppression of the Coulomb exchange has been found previously in different models of corresponding quantum dots arrays.

Finally, let us point out that the arrays of quantum dots or rings placed in photon cavities are in fact large and extended hybrid quantum systems, in contrast to smaller *qubit-like* devices (e.g. quantum dots coupled to microwave cavities [32, 33] or color centers coupled by phononic modes [34, 35]). The latter are extensively used

ACKNOWLEDGMENTS

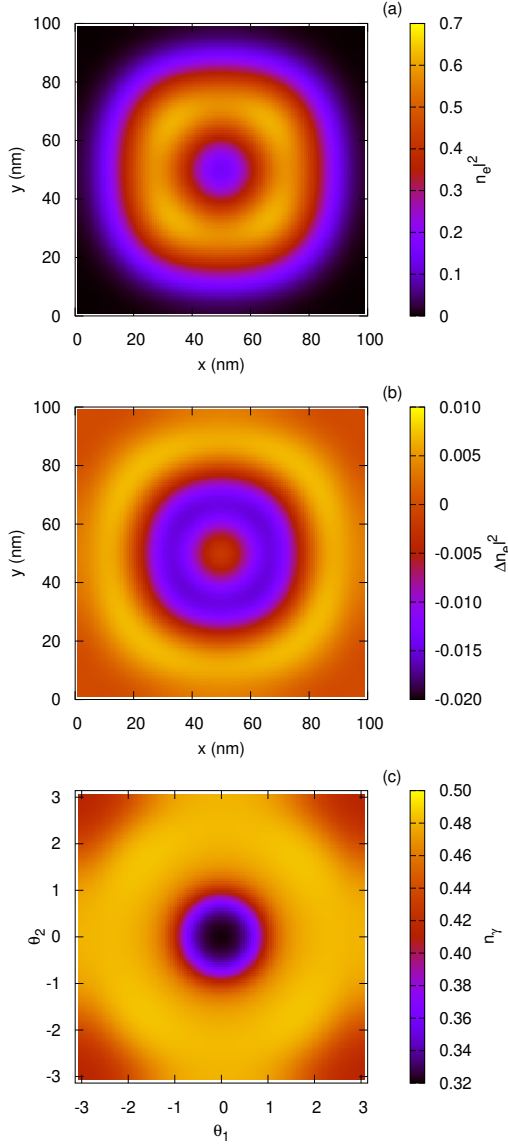


FIG. 5. The electron density $n_e l^2$ (a), the change in the electron density $\Delta n_e l^2 = [n_e(g_\gamma = 0.10) - n_e(g_\gamma = 0.01)]l^2$ (b), and the mean photon distribution $n_\gamma(\theta_1, \theta_2)$ in the reciprocal unit cell (c), see Eq. (15). $g_\gamma = 0.10$, $N_e = 3$, $pq = 2$, $E_\gamma = 0.70$ meV, $l = 28.21$ nm.

in quantum technologies, whereas the former provide important platforms merging collective effects and strong field-matter interaction. Note also that for large hybrid systems the theoretical tools and modeling are quite involved, as already illustrated in our present and previous studies based on QED-DFT and QED-DFT-TP methods.

This work was financially supported by the Research Fund of the University of Iceland grant No. 92199, and the Icelandic Infrastructure Fund for “Icelandic Research e-Infrastructure (IREI)”. The computations were performed on resources provided by the Icelandic High Performance Computing Center at the University of Iceland.

V. Mughnetsyan and V. Gudmundsson acknowledge support by the Higher Education and Science Committee of Armenia (grant No. 21SCG-1C012).

V. Gudmundsson acknowledges support for his visit to the National Taiwan University from the National Science and Technology Council, Taiwan under Grants No. NSTC 113-2811-M-002-001 and No. NSTC 112-2119-M-002-014.

H.-S.G. acknowledges support from the National Science and Technology Council, Taiwan under Grants No. NSTC 113-2112-M-002-022-MY3, No. NSTC 113-2119-M-002-021, No. NSTC 112-2119-M-002-014, No. NSTC 111-2119-M-002-007, and No. NSTC 111-2627-M-002-001, from the US Air Force Office of Scientific Research under Award Number FA2386-23-1-4052 and from the National Taiwan University under Grants No. NTU-CC-112L893404 and No. NTU-CC-113L891604. H.-S.G. is also grateful for the support from the “Center for Advanced Computing and Imaging in Biomedicine (NTU-113L900702)” through The Featured Areas Research Center Program within the framework of the Higher Education Sprout Project by the Ministry of Education (MOE), Taiwan, and the support from the Physics Division, National Center for Theoretical Sciences, Taiwan.

J.-D. Chai acknowledges support from the National Science and Technology Council, Taiwan under Grant No. NSTC 113-2112-M-002-032. J.-D. Chai is also grateful for the support from the Physics Division, National Center for Theoretical Sciences, Taiwan.

C.-S. Tang acknowledges funding support by the National United University through Contract No. 113-NUUPRJ-01.

V. Moldoveanu acknowledges financial support from the Core Program of the National Institute of Materials Physics, granted by the Romanian Ministry of Research, Innovation and Digitalization under the Project PC2-PN23080202.

Appendix A: Technical details in the methodology

For the calculations we use all the same parameters as is detailed in Appendix B in Ref. [22], except that in Figures 2, 5, and 6, we use the 16 lowest eigenstates of the photon number operator and a 32×32 nonequispaced grid in the first Brillouin zone of the reciprocal space, $\boldsymbol{\theta}$, built on a repeated 4-point Gaussian quadrature. This is done to guarantee the accuracy of the results for the static system for the electron-photon coupling $g_\gamma > 0.10$.

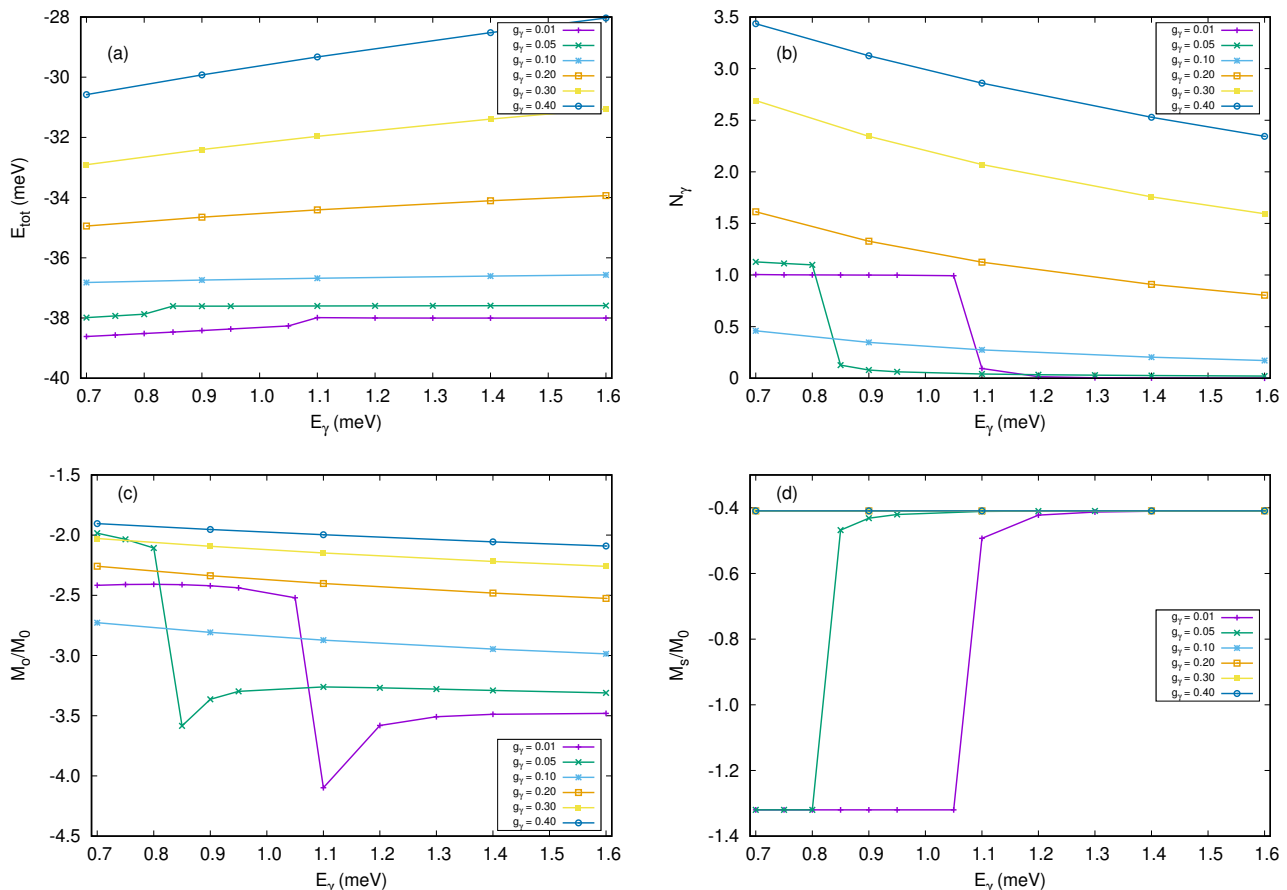


FIG. 6. The total energy E_{tot} (a), the mean number of photons N_γ (b), the orbital magnetization M_o (c), and the spin magnetization M_s (d) of the 2DEG in a unit cell as function of the photon energy E_γ for different values of the dimensionless electron-photon coupling g_γ . $T = 1.0$ K, $N_e = 3$, $pq = 2$, $M_0 = \mu_B^*/L^2$.

The ground state, or static, calculations are done in a linear functional basis constructed as a tensor product (TP) of electron and photon states $|\alpha\theta\sigma n\rangle = |\alpha\theta\sigma\rangle \otimes |n\rangle$. The electron states are states proposed by Ferrari [28], and used by Gudmundsson [30] and Silberbauer [29]. The photon states are the eigenstates of the photon number operator $N_\gamma = a_\gamma^\dagger a_\gamma$ with eigenvalue n . σ is the spin

label $\{\uparrow\downarrow\}$, and α is a composite quantum number for the Landau subband number.

The self-consistent diagonalization of the static total Hamiltonian leads to the states $|\alpha\theta\sigma n\rangle$, but the Liouville-von Neumann Eq. (11) is solved in the $\{|\alpha\theta\sigma n\rangle\}$ -basis as most matrix elements are known analytically there [22, 30].

-
- [1] J. Flick, H. Appel, M. Ruggenthaler, and A. Rubio, Cavity Born–Oppenheimer Approximation for Correlated Electron–Nuclear–Photon Systems, *Journal of Chemical Theory and Computation* **13**, 1616–1625 (2017).
- [2] J. Flick, N. Rivera, and P. Narang, Strong light-matter coupling in quantum chemistry and quantum photonics, *Nanophotonics* **7**, 1479–1501 (2018).
- [3] N. Tancogne-Dejean, M. J. T. Oliveira, X. Andrade, H. Appel, C. H. Borca, G. Le Breton, F. Buchholz, A. Castro, S. Corni, A. A. Correa, U. De Giovannini, A. Delgado, F. G. Eich, J. Flick, G. Gil, A. Gomez, N. Helbig, H. Hübener, R. Jestädt, J. Jornet-Somoza, A. H. Larsen, I. V. Lebedeva, M. Lüders, M. A. L. Marques, S. T. Ohlmann, S. Pipolo, M. Rampp, C. A. Rozzi, D. A. Strubbe, S. A. Sato, C. Schäfer, I. Theophilou, A. Welden, and A. Rubio, Octopus, a computational framework for exploring light-driven phenomena and quantum dynamics in extended and finite systems, *The Journal of Chemical Physics* **152** (2020), 124119.
- [4] F. Buchholz, I. Theophilou, S. E. B. Nielsen, M. Ruggenthaler, and A. Rubio, Reduced Density-Matrix Approach to Strong Matter-Photon Interaction, *ACS Photonics* **6**, 2694–2711 (2019).
- [5] J. A. Hutchison, T. Schwartz, C. Genet, E. Devaux, and T. W. Ebbesen, Modifying Chemical Landscapes by Coupling to Vacuum Fields, *Angewandte Chemie Interna-*

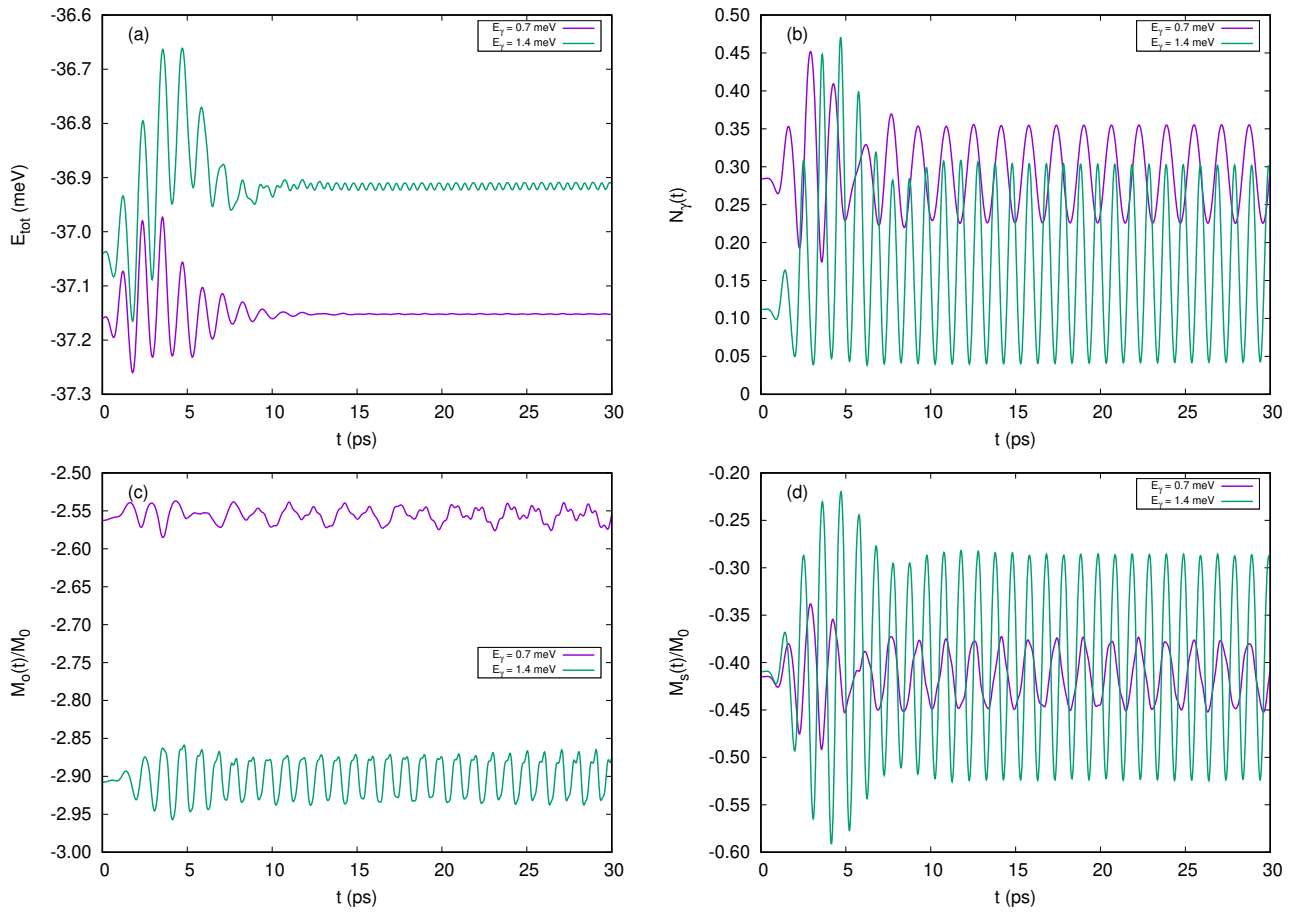


FIG. 7. The total energy E_{tot} (a), the mean number of photons N_γ (b), the orbital magnetization M_o (c), and the spin magnetization M_s (d) of the 2DEG in a unit cell as function of time for the first 30 ps for different values of the photon energy E_γ . $g_\gamma = 0.08$, $N_e = 3$, $pq = 2$, and $M_0 = \mu_B^*/L^2$.

tional Edition **51**, 1592–1596 (2012).

- [6] C. Schafer, J. Flick, E. Ronca, P. Narang, and Ángel Rubio, *Shining Light on the Microscopic Resonant Mechanism Responsible for Cavity-Mediated Chemical Reactivity* (2021).
- [7] J. Keller, G. Scalari, F. Appugliese, S. Rajabali, M. Beck, J. Haase, C. A. Lehner, W. Wegscheider, M. Failla, M. Myronov, D. R. Leadley, J. Lloyd-Hughes, P. Nataf, and J. Faist, Landau polaritons in highly nonparabolic two-dimensional gases in the ultrastrong coupling regime, *Phys. Rev. B* **101**, 075301 (2020).
- [8] J. Li, D. Golez, G. Mazza, A. J. Millis, A. Georges, and M. Eckstein, Electromagnetic coupling in tight-binding models for strongly correlated light and matter, *Phys. Rev. B* **101**, 205140 (2020).
- [9] J. Flick, C. Schäfer, M. Ruggenthaler, H. Appel, and A. Rubio, Ab Initio Optimized Effective Potentials for Real Molecules in Optical Cavities: Photon Contributions to the Molecular Ground State, *ACS Photonics* **5**, 992–1005 (2018), pMID: 29594185, <https://doi.org/10.1021/acsp Photonics.7b01279>.
- [10] J. Flick, Simple Exchange-Correlation Energy Functionals for Strongly Coupled Light-Matter Systems Based on the Fluctuation-Dissipation Theorem, *Phys. Rev. Lett.* **129**, 143201 (2022).
- [11] J. Malave, A. Ahrens, D. Pitagora, C. Covington, and K. Varga, Real-space, real-time approach to quantum-electrodynamical time-dependent density functional theory, *The Journal of Chemical Physics* **157** (2022), 194106.
- [12] D. B. Dar, A. Baranova, and N. T. Maitra, Reformulation of Time-Dependent Density Functional Theory for Nonperturbative Dynamics: The Rabi Oscillation Problem Resolved, *Phys. Rev. Lett.* **133**, 096401 (2024).
- [13] Q. Zhang, M. Lou, X. Li, J. L. Reno, W. Pan, J. D. Watson, M. J. Manfra, and J. Kono, Collective non-perturbative coupling of 2D electrons with high-quality-factor terahertz cavity photons, *Nature Physics* **12**, 1005 (2016).
- [14] G. Scalari, C. Maissen, D. Turčinková, D. Hagenmüller, S. D. Liberato, C. Ciuti, C. Reichl, D. Schuh, W. Wegscheider, M. Beck, and J. Faist, Ultrastrong Coupling of the Cyclotron Transition of a 2D Electron Gas to a THz Metamaterial, *Science* **335**, 1323–1326 (2012).
- [15] V. Rokaj, M. Ruggenthaler, F. G. Eich, and A. Rubio, Free electron gas in cavity quantum electrodynamics, *Phys. Rev. Res.* **4**, 013012 (2022).
- [16] V. Rokaj, M. Penz, M. A. Sentef, M. Ruggenthaler, and A. Rubio, Quantum Electrodynamical Bloch Theory with Homogeneous Magnetic Fields, *Phys. Rev. Lett.* **123**,

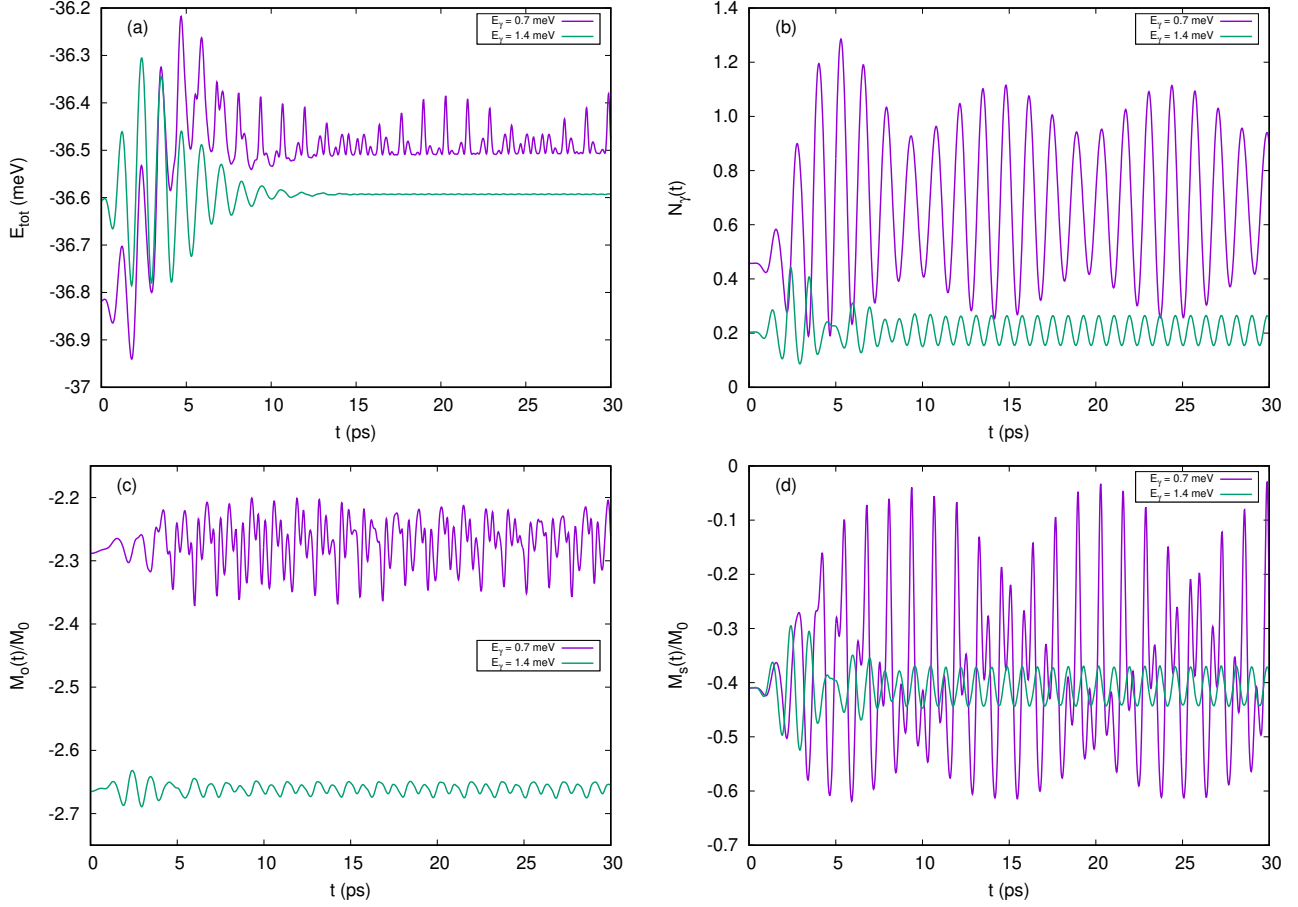


FIG. 8. The total energy E_{tot} (a), the mean number of photons N_γ (b), the orbital magnetization M_o (c), and the spin magnetization M_s (d) of the 2DEG in a unit cell as a function of time for the first 30 ps for different values of the photon energy E_γ . $g_\gamma = 0.10$, $N_e = 3$, $pq = 2$, and $M_0 = \mu_B^*/L^2$.

- 047202 (2019).
- [17] V. Rokaj, M. Penz, M. A. Sentef, M. Ruggenthaler, and A. Rubio, Polaritonic Hofstadter butterfly and cavity control of the quantized Hall conductance, *Phys. Rev. B* **105**, 205424 (2022).
- [18] V. Gudmundsson, V. Mughnetsyan, N. R. Abdullah, C.-S. Tang, V. Moldoveanu, and A. Manolescu, Effects of a far-infrared photon cavity field on the magnetization of a square quantum dot array, *Phys. Rev. B* **106**, 115308 (2022).
- [19] V. Mughnetsyan, V. Gudmundsson, N. R. Abdullah, C.-S. Tang, V. Moldoveanu, and A. Manolescu, Magnetic Properties of A Cavity-Embedded Square Lattice of Quantum Dots or Antidots, *Annalen der Physik* **536**, 2300274 (2024).
- [20] V. Gudmundsson, V. Mughnetsyan, H.-S. Goan, J.-D. Chai, N. R. Abdullah, C.-S. Tang, V. Moldoveanu, and A. Manolescu, Magneto-optical properties of a quantum dot array interacting with a far-infrared photon mode of a cylindrical cavity, *Phys. Rev. B* **109**, 235306 (2024).
- [21] V. Gudmundsson, V. Mughnetsyan, N. R. Abdullah, C.-S. Tang, V. Moldoveanu, and A. Manolescu, Controlling the excitation spectrum of a quantum dot array with a photon cavity, *Phys. Rev. B* **108**, 115306 (2023).
- [22] V. Gudmundsson, V. Mughnetsyan, H.-S. Goan, J.-D. Chai, N. R. Abdullah, C.-S. Tang, V. Moldoveanu, and A. Manolescu, Tuning of paramagnetic and diamagnetic cavity photon excitations in a square array of quantum dots in a magnetic field, *Phys. Rev. B* **110**, 205301 (2024).
- [23] M. I. Lubin, O. Heinonen, and M. D. Johnson, Spin-ensemble density-functional theory for inhomogeneous quantum Hall systems, *Phys. Rev. B* **56**, 10373–10382 (1997).
- [24] M. Koskinen, M. Manninen, and S. M. Reimann, Hund's Rules and Spin Density Waves in Quantum Dots, *Phys. Rev. Lett.* **79**, 1389–1392 (1997).
- [25] U. von Barth and L. Hedin, A local exchange-correlation potential for the spin polarized case. i, *Journal of Physics C: Solid State Physics* **5**, 1629–1642 (1972).
- [26] B. Tanatar and D. M. Ceperley, Ground state of the two-dimensional electron gas, *Phys. Rev. B* **39**, 5005–5016 (1989).
- [27] R. D. Hofstadter, Energy levels and wave functions of Bloch electrons in rational and irrational magnetic fields, *Phys. Rev. B* **14**, 2239 (1976).
- [28] R. Ferrari, Two-dimensional electrons in a strong magnetic field: A basis for single-particle states, *Phys. Rev. B* **42**, 4598 (1990).
- [29] H. Silberbauer, Magnetic minibands in lateral semicon-

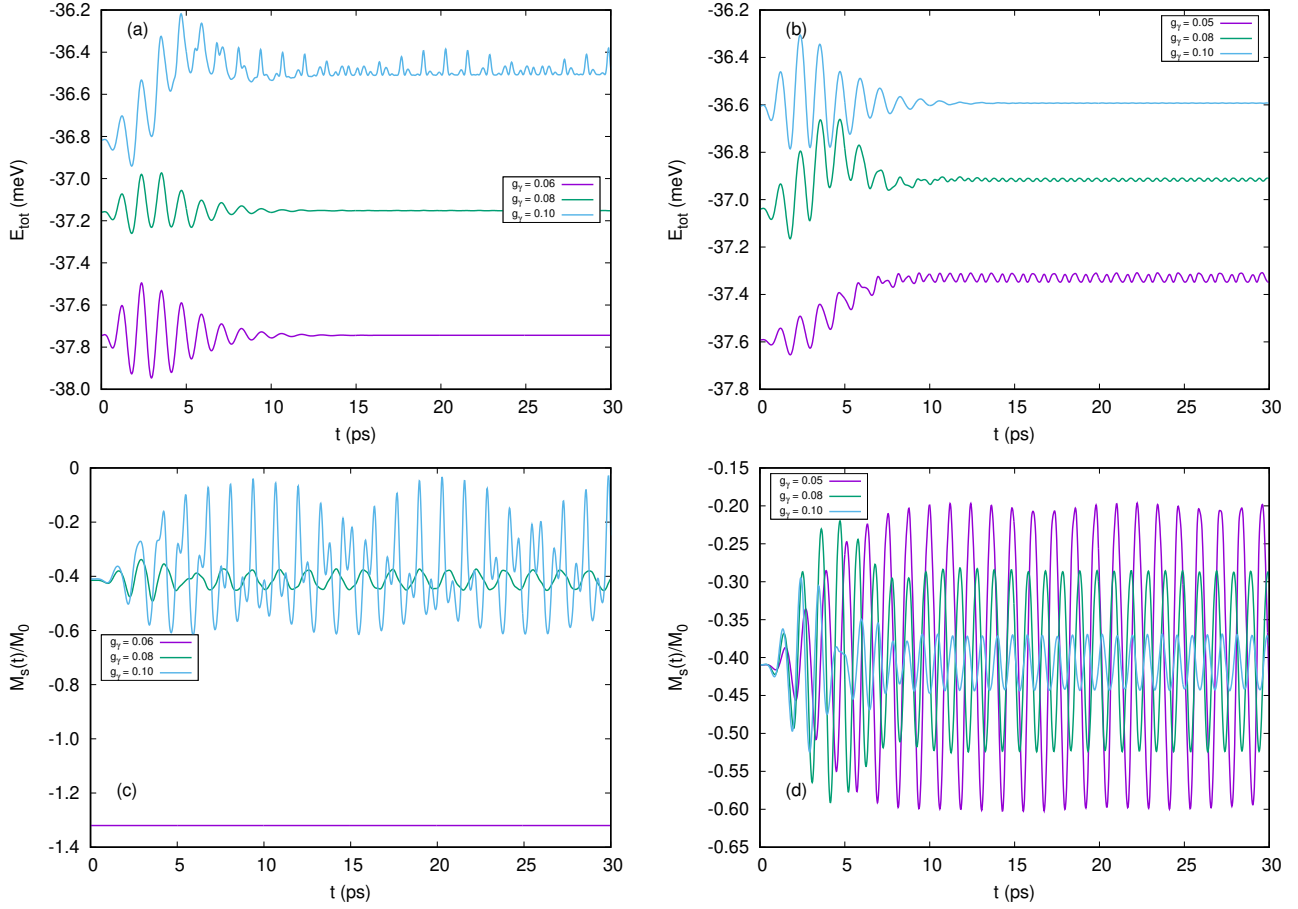


FIG. 9. The total energy E_{tot} for the photon energy $E_\gamma = 0.70$ meV (a), $E_\gamma = 1.40$ meV (b), and the spin magnetization M_s for $E_\gamma = 0.70$ meV (c), $E_\gamma = 1.40$ (d) of the 2DEG in a unit cell as function of time for the first 30 ps for different values of the electron-photon coupling g_γ . $N_e = 3$, $pq = 2$, and $M_0 = \mu_B^*/L^2$.

- ductor superlattice, *J. Phys. C* **4**, 7355 (1992).
- [30] V. Gudmundsson and R. R. Gerhardts, Effects of screening on the Hofstadter butterfly, *Phys. Rev. B* **52**, 16744 (1995).
- [31] D. Pfannkuche, V. Gudmundsson, and P. Maksym, Comparison of a Hartree, a Hartree-Fock, and an Exact Treatment of Quantum Dot Helium, *Phys. Rev. B* **47**, 2244 (1993).
- [32] A. Stockklauser, P. Scarlino, J. V. Koski, S. Gasparinetti, C. K. Andersen, C. Reichl, W. Wegscheider, T. Ihn, K. Ensslin, and A. Wallraff, Strong Coupling Cavity QED with Gate-Defined Double Quantum Dots Enabled by a High Impedance Resonator, *Phys. Rev. X* **7**, 011030 (2017).
- [33] P. Scarlino, J. H. Ungerer, D. J. van Woerkom, M. Mancini, P. Stano, C. Müller, A. J. Landig, J. V. Koski, C. Reichl, W. Wegscheider, T. Ihn, K. Ensslin, and A. Wallraff, In situ Tuning of the Electric-Dipole Strength of a Double-Dot Charge Qubit: Charge-Noise Protection and Ultrastrong Coupling, *Phys. Rev. X* **12**, 031004 (2022).
- [34] F. Fung, E. Rosenfeld, J. D. Schaefer, A. Kabcenell, J. Gieseler, T. X. Zhou, T. Madhavan, N. Aslam, A. Yacoby, and M. D. Lukin, Toward Programmable Quantum Processors Based on Spin Qubits with Mechanically Mediated Interactions and Transport, *Phys. Rev. Lett.* **132**, 263602 (2024).
- [35] C. E. Bradley, J. Randall, M. H. Abobeih, R. C. Berrevoets, M. J. Degen, M. A. Bakker, M. Markham, D. J. Twitchen, and T. H. Taminiau, A Ten-Qubit Solid-State Spin Register with Quantum Memory up to One Minute, *Phys. Rev. X* **9**, 031045 (2019).